AD-A171 056 STRESS IN A BONDED WAFER(U) NAVAL RESEARCH LAB WASHINGTON DC V J PARKS 23 JUN 86 NRL-MR-5809 1/1

UNCLASSIFIED F/G 20/11 NL

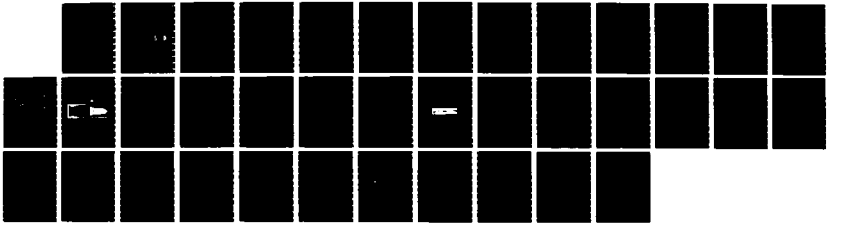

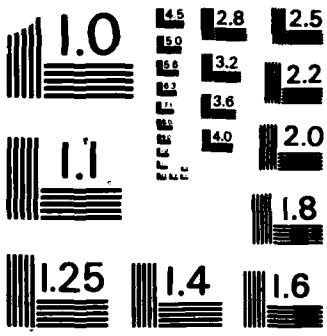

MICROCOPY RESOLUTION TEST CHART
NATIONAL BUREAU OF STANDARDS - 1963 - A

AD-A171 056

Stress in a Bonded Wafer

V. J. PARKS

Structural Integrity Branch
Marine Technology Division

Prepared for

Sandia National Laboratories
Albuquerque, New Mexico

DTIC
ELECTE
AUG 1 4 1986
S D

DTIC FILE COPY

Approved for public release; distribution unlimited

AD-A170 056

SECURITY CLASSIFICATION OF THIS PAGE

REPORT DOCUMENTATION PAGE

1a REPORT SECURITY CLASSIFICATION UNCLASSIFIED	1b RESTRICTIVE MARKINGS
2a SECURITY CLASSIFICATION AUTHORITY	3 DISTRIBUTION / AVAILABILITY OF REPORT Approved for public release, distribution unlimited.
2b DECLASSIFICATION / DOWNGRADING SCHEDULE	
4 PERFORMING ORGANIZATION REPORT NUMBER(S) NRL Memorandum Report 5809	5 MONITORING ORGANIZATION REPORT NUMBER(S)
6a NAME OF PERFORMING ORGANIZATION Naval Research Laboratory 6b OFFICE SYMBOL (If applicable) Code 5832	7a NAME OF MONITORING ORGANIZATION
6c ADDRESS (City, State, and ZIP Code) Washington, DC 20375	7b ADDRESS (City, State, and ZIP Code)
8a NAME OF FUNDING / SPONSORING ORGANIZATION Sandia National Laboratories 8b OFFICE SYMBOL (If applicable) Division 1846	9 PROCUREMENT INSTRUMENT IDENTIFICATION NUMBER
8c ADDRESS (City, State, and ZIP Code) Albuquerque, New Mexico 87185	10 SOURCE OF FUNDING NUMBERS PROGRAM ELEMENT NO. / PROJECT NO. / TASK NO / WORK UNIT ACCESSION NO. DN156-191

11 TITLE (Include Security Classification)

Stress in a Bonded Wafer

12 PERSONAL AUTHOR(S)

Parks, Vincent J.

13a TYPE OF REPORT	13b TIME COVERED	14 DATE OF REPORT (Year, Month, Day)	15 PAGE COUNT
Final	FROM Oct 84 TO Oct 85	1986 June 23	37

16 SUPPLEMENTARY NOTATION

17 COSATI CODES			18 SUBJECT TERMS (Continue on reverse if necessary and identify by block number)
FIELD	GROUP	SUB-GROUP	

19 ABSTRACT (Continue on reverse if necessary and identify by block number)

Stresses in a flat wafer, bonded on both sides to rods of another material and subjected to axial forces perpendicular to the bonded surfaces, are treated both experimentally and theoretically. A two dimensional model analysis of the axial meridian plane of the wafer shows the build-up of stresses in the corners where the bonded surfaces meet the free surface between the rods. A three dimensional model analysis of the wafer shows a similar build-up of stresses in the corners. The principal point of these analyses is that the stress build-up drops off to a uniform stress field within two wafer thicknesses from the free surface.

A theoretical analysis obtains the uniform stress field that acts on the wafer beyond two thicknesses of the free surface. This theoretical solution is shown to also give the stresses due to uniform changes in temperature of the wafer and the rods, where the wafer material and the rod material have different coefficients of thermal expansion.

20 DISTRIBUTION / AVAILABILITY OF ABSTRACT ☐ UNCLASSIFIED/UNLIMITED ☒ SAME AS RPT ☐ DTIC USERS	21 ABSTRACT SECURITY CLASSIFICATION UNCLASSIFIED
22a NAME OF RESPONSIBLE INDIVIDUAL Vincent J. Parks	22b TELEPHONE (Include Area Code) (202) 767-3384 22c OFFICE SYMBOL Code 5832

DD FORM 1473, 84 MAR 83 APR edition may be used until exhausted
All other editions are obsolete

SECURITY CLASSIFICATION OF THIS PAGE

CONTENTS

QUALITY INSPECTED 1

Accesion For	
NTIS CRA&I	☒
DTIC TAB	☐
Unannounced	☐
Justification	
By	
Dist. ibution /	
Availability Codes	
Dist	Avail and / or Special
A-1	

STRESS IN A BONDED WAFER

INTRODUCTION

Joining two structural parts with adhesive is common engineering practice. The joint is often used to transmit a force between the parts. Such a force generates stresses in the parts and in the adhesive layer. If the mechanical properties of the structural parts are markedly different from the mechanical properties of the adhesive, the stress system at the adhesive interfaces becomes complex.

This is a report on the stresses due to forces normal to a flat adhesive layer. The experimental testing was restricted to an approximately constant thickness layer between two circular bars subjected to axial load (see Fig. 1 and Ref 1). Because the adhesive layer has the form of a thin circular disk, it is termed a bonded wafer. This study is prompted by the interest in a glass wafer between metal bars. However, many of the results can be applied to other materials and geometries.

PREVIOUS THEORETICAL ANALYSIS

The stress analysis of a wafer under axial load is reviewed by Adams et al (2). They point out that the simplest analysis assumes no strains perpendicular to the axis, in either the wafer or the adjoining parts. This gives a stress ratio, in terms of the adhesive's Poisson's ratio, (νa) of

$$\frac{\sigma_h}{\sigma} = \frac{\nu_a}{1-\nu_a} \qquad (1)$$

where σ is the applied vertical stress and σ_h is the generated horizontal stress.

They further point out that, using Kuenzi & Stevens' (3) assumption of lateral contraction (Poisson's effect) in the adjoining parts, this stress ratio comes out to be somewhat less

$$\frac{\sigma_h}{\sigma} = \frac{\nu_a - (E_a/E_p)\nu_p}{1-\nu_a} \qquad (2)$$

where Ea and Ep are the elastic moduli of the adhesive and adjoining parts, respectively. Adams et al make clear that this solution assumes a uniform horizontal stress over the whole of both interface surfaces and neglects shear stresses that must

Manuscript approved April 17, 1986.

exist near the free boundary. To supplement this solution they conducted a finite element analysis that shows the uniformity of normal stresses (both horizontal and vertical) in the central region, and the analysis also shows the variation of normal stresses near the edge, along with the build-up of shear stresses. The work of Adams et al is reviewed by Kinloch (4).

THEORETICAL ANALYSIS REPORTED HERE

The stress analysis in the three references cited above (2,3,4) emphasizes application to adhesives which are much softer than the adjoining parts. As the adhesive approaches (or passes) the stiffness of the adjoining parts, there are additional strains put on both the adhesive and the adjoining parts. The stress analysis of an interface, far from the edge, of two dissimilar materials, of any stiffness, bonded on a flat plane and loaded uniformly perpendicular to the plane, is presented in the appendix. This analysis applies to the central region of the wafer and extends the solution given in Eqn. (2) to all stiffnesses. From Eqn A-10 the horizontal stress ratio is

$$\frac{\sigma_h}{\sigma} = \frac{\nu_a - (E_a/E_p)\,\nu_p}{1 - \nu_a + (E_a/E_p)(1-\nu_p)} \qquad (3)$$

Note that for very low values of Ea/Ep Eqn (3) agrees with Eqn (2), and even Eqn (1).

To conduct a stress analysis in the central region of a thin wafer, Eqn (3) can be used by dividing the load by the cross sectional area of the wafer to obtain the vertical stress. This gives σ. Using the material properties of the wafer (E_a, ν_a) and the material properties of the adjoining parts (E_p, ν_p) the horizontal stresses, which act in all horizontal directions, can be obtained . This gives a complete stress tensor ($\sigma, \sigma_h, \sigma_h$) at all points in the central region of the wafer, both on the interfaces, and between the interfaces.

Equations (1) to (3) are specified as acting only in the "central" region of the adhesive wafer. This central region can be taken as all of the wafer beyond several wafer thicknesses from the free edge of the wafer. So to use these equations, the wafer thickness can be no more than about 1/4 of the wafer diameter, and the thinner the wafer becomes, with respect to the diameter, the larger the portion of the wafer for which Eqns (1, 2 and 3) apply.

EXPERIMENTAL ANALYSIS

In order to complete the stress analysis, it is necessary to obtain the stresses near the free edge of the wafer. This requires additional, and more elaborate, analysis. The finite element method used by Adams et al is one approach. The method, once set up, can provide a number of solutions, with a wide variation of material properties, and various thickness-to-width

ratios. If there is a weakness in the method, as applied to the wafer problem, the weakness is that the maximum stress is concentrated at a point , the sharp corner at the free edges of the interfaces. The finite element method can only approximate the stress at this point, by the use of smaller and smaller size elements.

Alternatively, an analysis which physically measures the stress at the corners is the photoelastic model analysis of the wafer. Of course, this method has its own limitatioins to be discussed below.

TWO-DIMENSIONAL ANALYSIS

A two-dimensional photoelastic analysis of the problem was conducted by Mylonas (5). Figure 2 shows patterns and plots obtained from that study. Mylonas noted a serious difficulty of the two-dimensional approach. In order to be applied to the plane strain case, the two-dimensional model must be in a state of plane stress, with no stresses perpendicular to the model surfaces. However, as Mylonas shows, the bonded interface generates out-of-plane stresses when loaded. The many fringes along the bonded surfaces in Fig. 2 emphasize this condition. Indeed, the bonded surface is in a state of plane strain. So the two-dimensional model of a bonded interface is a hybrid model, half plane-stress, half plane-strain, and validly representing neither case.

Figure 3 shows the photoelastic patterns of a two dimensional strip model which attempt to achieve a plane stress condition along the bonded edges by bonding to a knives so that there is no out-of-plane restraint, and thus no out-of-plane stress. The high build-up of fringes along the bonded edge seen in Fig. 2 has been eliminated, but, it is not certain that the stress build-up at the corners is quantitatively exact. Despite these questions, the fringe patterns do indicate the stress distribution in the wafer.

The strip model shown in Fig. 3 is loaded by a thermal shrinkage produced during curing of the model material on the knife edges. In the Appendix, the correspondence between stresses on a wafer subjected to load (Eqn A-10) and the stresses due to thermal shrinkage (Eqn A-11) is indicated. This correspondence is developed below for the 2-D and 3-D cases. The strain optic law for photoelastic materials is

$$\epsilon_1 - \epsilon_2 = 2 n F_\epsilon \qquad (4)$$

where ϵ_1, and ϵ_2 are the principal strains in the plane perpendicular to the direction of view, n is the fringe order at the point of strains ϵ_1 and ϵ_2, and F_ϵ is the photoelastic model constant.

The model constant can be obtained directly from the strip model since a fringe order n_o, and the principal strains in terms of the shrinkage are known in the central region. The horizontal strain $\epsilon_1 = \alpha$, and the vertical strain $\epsilon_2 = -\nu\alpha$. Using these values to solve for F_ϵ,

$$F_\epsilon = (\alpha - (-\nu\alpha)) / 2n_o.$$

the strain optic law can then be written

$$\epsilon_1 - \epsilon_2 = \frac{n}{n_o}(1+\nu)\alpha. \tag{5}$$

or if the strains are taken in a normalized form

$$\frac{\epsilon_1}{\alpha} - \frac{\epsilon_2}{\alpha} = \frac{n}{n_o}(1+\nu). \tag{6}$$

This use of a known strain (or stress) somewhere on the model is sometimes referred to as autocalibration.

The cartesian normal and shear strains are related to the principal strains as follows:

$$\frac{\epsilon_x}{\alpha} - \frac{\epsilon_y}{\alpha} = \left(\frac{\epsilon_1}{\alpha} - \frac{\epsilon_2}{\alpha}\right)\cos 2\theta \tag{7}$$

$$\frac{\gamma_{xy}}{\alpha} = \left(\frac{\epsilon_1}{\alpha} - \frac{\epsilon_2}{\alpha}\right)\sin 2\theta$$

where ϵ_x and ϵ_y are the normal strains and γ_{xy} is the cartesian shear strain at the same point at which ϵ_1 and ϵ_2 are acting, and θ is the direction of the principal strain with respect to the cartesian direction.

Thus, the cartesian strains can be written in terms of the photoelastic data

$$\frac{\epsilon_x}{\alpha} - \frac{\epsilon_y}{\alpha} = \frac{n}{n_o}(1+\nu)\cos 2\theta \tag{8}$$

$$\frac{\gamma_{xy}}{\alpha} = \frac{n}{n_o}(1+\nu)\sin 2\theta$$

Both n and n_o can be taken directly from the pattern shown in Fig. 3. The value of θ is obtained by rotating the polariscope until the point of analysis darkens. So all the variables on the right hand side of Eqn (8) are available from the photoelastic patterns.

Along the interface between the strip and the knife edge, the strain tangential to the knife edge must be equal to the free

shrinkage, just as it is everywhere in the central region. Calling the direction of the knife edge, the x-direction

$$\epsilon_x = \alpha \quad \text{or} \quad \frac{\epsilon_x}{\alpha} = 1 \tag{9}$$

and Eqn (8) reduces to

$$\begin{aligned} \epsilon_y/\alpha &= 1 - (n/n_0)(1+\nu)\cos 2\theta \\ \gamma_{xy}/\alpha &= (n/n_0)(1+\nu)\sin 2\theta \end{aligned} \tag{10}$$

The photoelastic variables n and θ along the knife edge are plotted in Fig. 4, n_0 is 0.71. Since $\epsilon x/\alpha = 1$, all the normalized strains along the knife are determined. From the two-dimensional form of Hooke's Law, the stresses in this same normalized form can be determined.

$$\begin{aligned} \sigma_x/E\alpha &= \frac{1}{1-\nu^2}(\epsilon_x/\alpha + \nu\,\epsilon_y/\alpha) \\ \sigma_y/E\alpha &= \frac{1}{1-\nu^2}(\epsilon_y/\alpha + \nu\,\epsilon_x/\alpha) \\ \tau_{xy}/E\alpha &= (\gamma_{xy}/\alpha)/2(1+\nu) \end{aligned} \tag{11}$$

The cartesian stresses along the knife edge are plotted in Fig. 5.

As indicated in the appendix, these stresses have the same distribution as the stresses due to pinching in the wafer problem. The shrinkage load in terms of the horizontal stress is $E\alpha$. The corresponding pinching load on the wafer is $\nu\sigma$, where ν is Poisson's ratio of the strip material. Thus, to convert from shrinkage load to pinching load it is necessary to replace $E\alpha$ with $\nu\sigma$.

Replacing $E\alpha$ with the $\nu\sigma$ in Eqn (11) would normalize the stresses in terms of $\nu\sigma$. To normalize the stresses in terms of σ it is necessary to multiply the values obtained from the right side of Eqn 11 (and plotted in Fig. 5) by ν. Further, in order to complete the stress field, it is necessary to add the axial stress field ($\sigma_y = \sigma$) to the pinching stress field obtained from the shrinkage field. So the stress values shown in Fig 5 have all been multiplied by ν (=0.48) and the σy values all increased by ($\sigma y/\sigma = 1$). The two-dimensional stress field in the strip bonded on its edges and subjected to uniaxial load is shown in Fig 6. Note the shear stresses are just reduced by about one half and the normal stresses (σx and σy) more or less change places. To complete the picture, the principal stresses are obtained using the standard tensor transformation equations and are plotted in Fig. 7 along the maximum shear stress.

The transformation equations are:

$$\sigma_1, \sigma_2 = \frac{1}{2}(\sigma_x + \sigma_y) \pm \sqrt{\frac{1}{4}(\sigma_x - \sigma_y)^2 + \tau_{xy}^2} \qquad (12)$$

$$\tau_{max} = \sqrt{\frac{1}{4}(\sigma_x - \sigma_y)^2 + \tau_{xy}^2}$$

The stresses given in Figs 5 and 7 are "plane stress" stresses. In the case of first boundary value problems these stresses would apply rigorously to the "plane strain" case. Because the wafer problem is a mixed boundary value problem, the plane stresses apply to the plane strain case for which

$$\nu_1 = \frac{\nu}{1 + \nu} \qquad (13)$$

where ν_1, is Poisson's ratio of the material in plane strain and ν is Poisson's ratio of the material in plane stress.

For $\nu = 0.48$ in plane stress, the analysis applies rigorously to a material in plane strain with $\nu_1 = 0.324$.

Finally, because the regions of interest (the corners) are at and near the ends of the plane stress and plane strain bodies, the analysis can be extended to a square body and to the round axisymmetric case. This chain of applications, from the 2-D shrinkage strip model to the 3-D axisymmetric bonded wafer is shown in Fig. 8.

The main point, through all of this, as the data shows, is that the stresses drop off to the values described in the theoretical section, within about 2 wafer thicknesses from the boundary.

THREE-DIMENSIONAL EXPERIMENTAL ANALYSIS

Three-dimensional photoelasticity provides a direct physical measurement of stress in a wafer. This method also has its limitations. First, it is difficult to model various material property ratios. Second, because of meniscus and shrinking effects, the corner of the cast model is never completely square. Third, and most important (as in the two-dimensional modeling), the thermal changes which occur in three-dimensional photoelasticity when applied to bonded interfaces, create thermal stresses, in addition to those stresses of interest (the mechanical stresses due to load).

These thermal stresses, as in the two-dimensional case occur in part during curing. However, the three-dimensional photoelastic analysis requires heating the model to "freeze-in" the stresses so that the model can be disected at room temperature to view the stress pattern. Thus, thermal stresses are inherent in three-dimensional photoelastic analysis of bonded bodies.

After several attempts to minimize the thermal stresses and maximize the axial load stresses, it was decided to use the same transformation technique used in the two-dimensional analysis to obtain the load stress distribution from the analysis of the shrinkage stress field. To simplify the modeling, it was also decided to bond the wafer on one side only, thus representing a half wafer. Since the shrinkage load cannot create any overall axial force, no significant axial stresses were expected in the midplane of the wafer. This has been shown to be the case in the two-dimensional models, by cutting them in half, lengthwise.

Figure 9 is the photoelastic pattern in a slice cut from a wafer which was cast, bonded, and shrunk on a thick steel disk. Figure 10 shows the photoelasticity variables, n and θ along the interface of the wafer. Figure 11 gives the normalized cartesian stresses, along the interface, obtained from a development of Eqn (8) similar to the 2-D approach, except that in the 3-D case the strains on and tangential to the interface are assumed equal to α in all directions (both x and Z). The principal stresses calculated from Eqn (12) are plotted in Fig. 12.

The main differences from the 2-D analysis is the increase in normal stresses near the end of the interface, and the fact that at each point the principal stresses are almost the same. Both these differences are due to the high Poisson's ratio of the wafer material ($\nu = 0.48$) and the high Young's modulus ratio of the model base material to model wafer material. Despite these differences, the results indicate the main point in this report, that the strains, and stresses, drop off to a uniform value, within several thicknesses from the free boundary of the wafer.

DISCUSSION OF WAFER FAILURE

Despite the fact that the maximum stress has been shown to occur and does occur at the edge of the wafer interface, most failures occur in the central region on one of the interfaces. The seeming contradiction is due to at least three factors. First, the central region is in a triaxial state of stress whereas the corner, at the intersection of the interface and the free edge, is in a biaxial state of stress. Second, the volume under the triaxial stress is larger than the volume under the biaxial stress. The third, not so obvious, factor is suggested by Eqn (A-11) in the appendix. That equation shows that the thermal contradiction (and curing shrinkage), that occurs during curing of the adhesive, sets up interior horizontal stresses. So there is a significant state of uniform biaxial tension on the wafer before any axial load is ever applied. This third factor needs some qualification. As seen Fig. 11, the curing shrinkage does create some axial tensile strain near the corner in addition to the biaxial horizontal tension in the interior. This additional corner stress must be considered in terms of the first two factors (it's non-triaxial nature, and it's small volume of extent).

CONCLUSIONS

A rigorous solution has been found for the stresses in the central region of a bonded wafer under axial load, and also for the same wafer subjected to uniform thermal (or curing) shrinkage.

Model analysis demonstrates that the stresses away from the free boundary of the loaded wafer decay to the value of stresses in the central region, within a few wafer thicknesses from the boundary.

REFERENCES

1. ASTM D2095-72 (Reapproved 1978), "Standard Test Method for Tensile Strength of Adhesives by Means of Bar and Rod Specimens," Annual Book of American Society for Testing Materials Standards, Part 22.

2. Adams, R.D., Coppendale, J., and Peppiatt, N.A., "Stress Analysis of Axisymmetric Butt Joints Loaded in Torsion and Tension," Journal of Strain Analysis, Vol. 13, No. 1, p. 1, 1978.

3. Kuenzi, E.W. and Stevens, G.H., "Determination of Mechanical Properties of Adhesives for Use in the Design of Bonded Joints," Forest Products Laboratory, Report FPL-011, 1963, AD418993.

4. Kinloch, A.J., "The Science of Adhesion, Part 2 Mechanics and Mechanisms of Failure," Journal of Materials Science, Vol. 17, p. 617, 1982.

5. Mylonas, C., "Experiments on Composite Models with Applications to Cemented Joints," Proceeding of the Society for Experimental Stress Analysis, Vol. XII, No. 2. 1955.

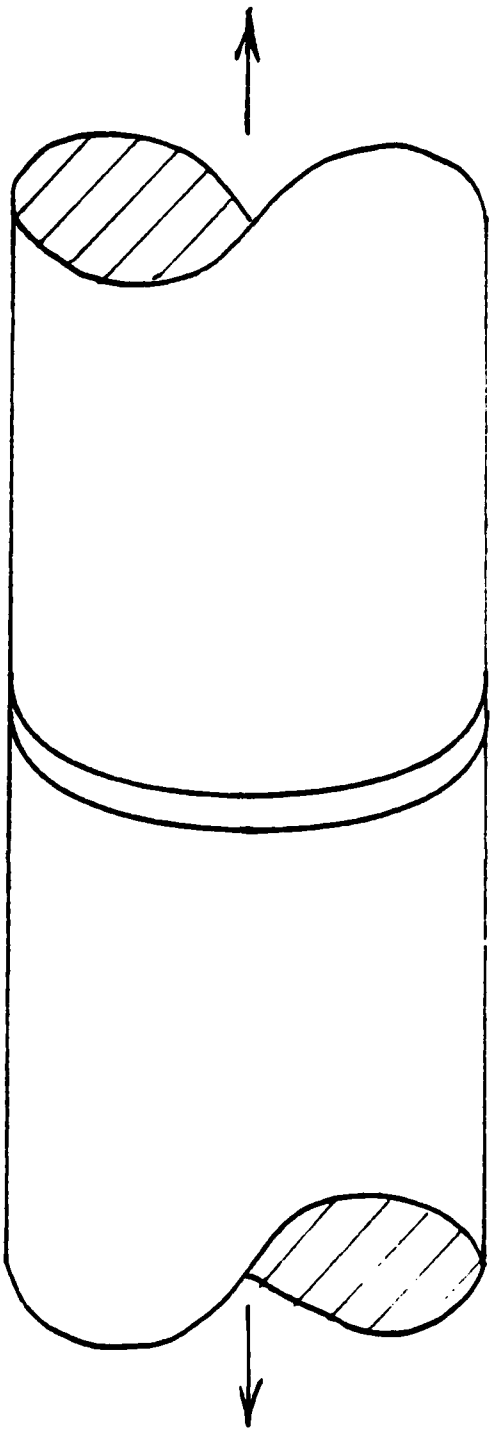

Fig. 1 — Geometry of bonded wafer under uniaxial load

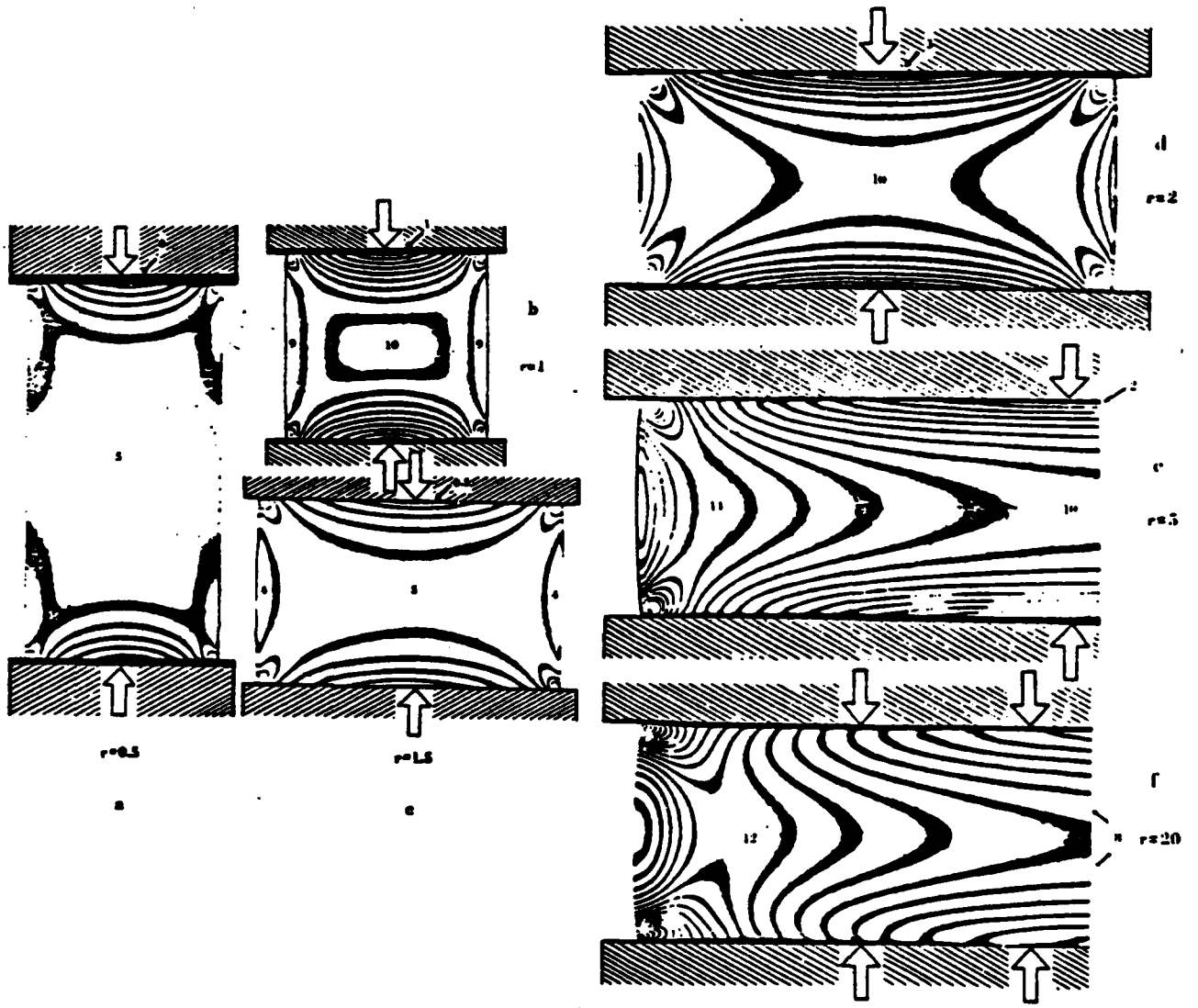

Fig. 2 — Two-dimensional photoelastic patterns of strips of various width-to-height ratios (r) bonded on the upper and lower edges and subjected to uniaxial force. The fringes on the bonded edges of all the models indicate out-of-plane restraint due to the bonding (drawn from Reference 5)

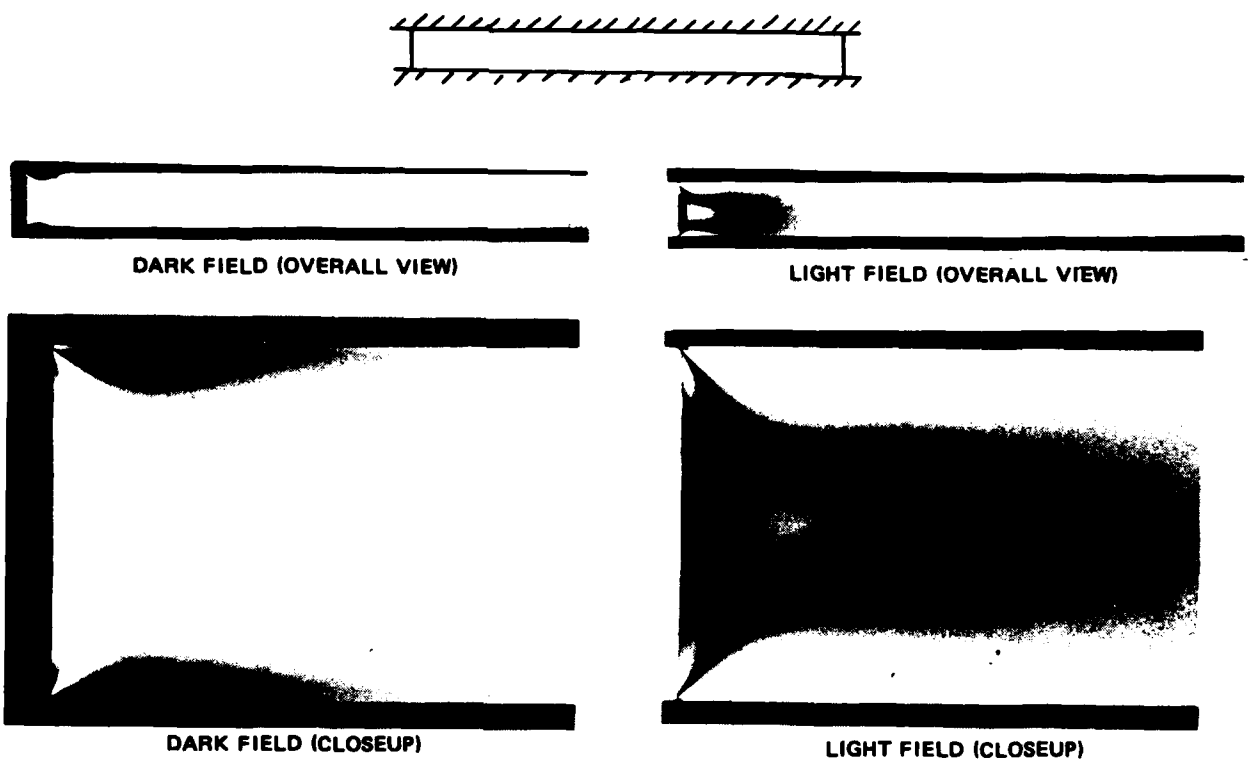

Fig. 3 — Isochromatic fringes on rubber strip indicating local nature of stress build-up in the corners near the free end of the strip

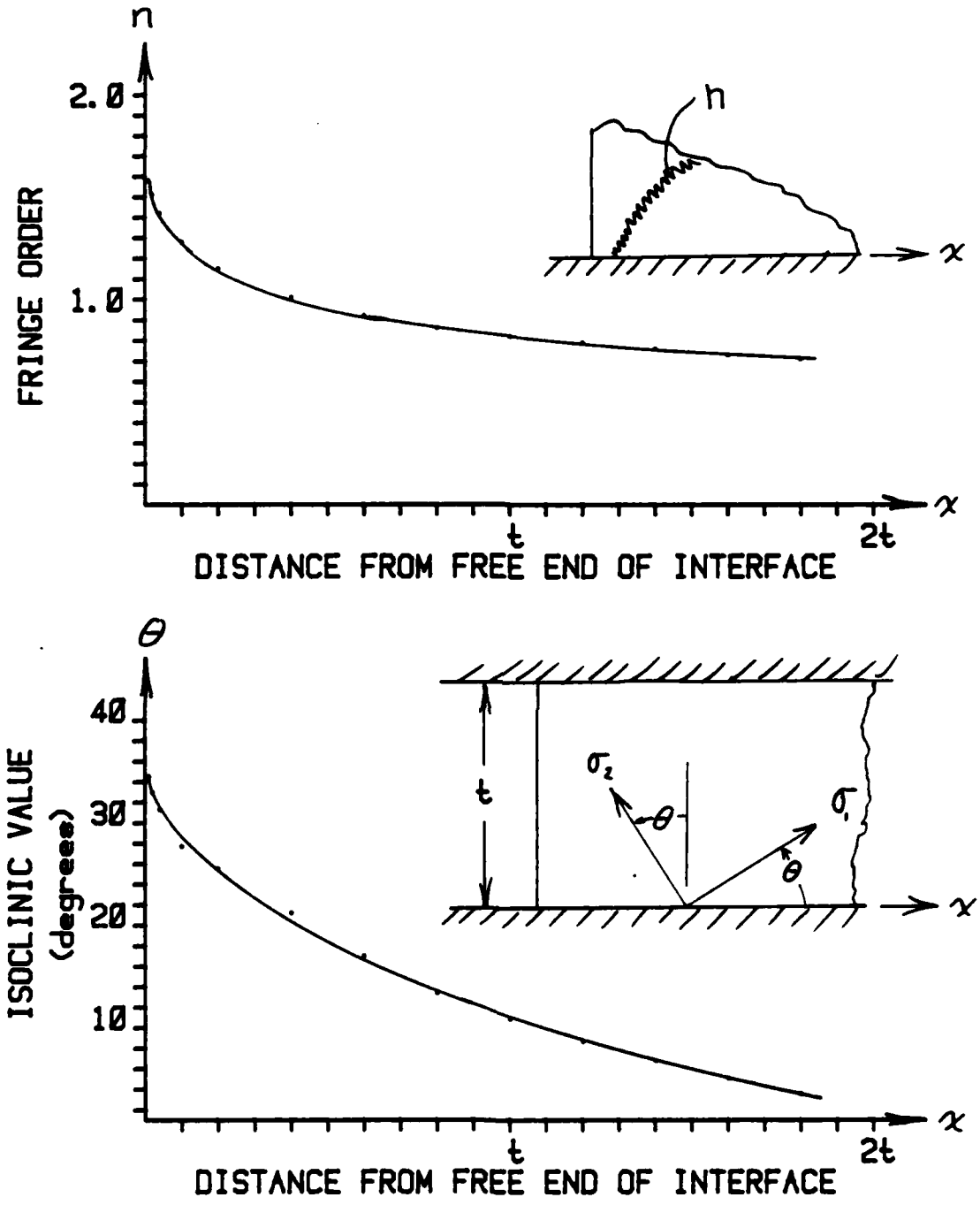

Fig. 4 — Isochromatic fringes and isoclinic values along model interface near free edge. Isoclinics show the direction of the principal stresses.

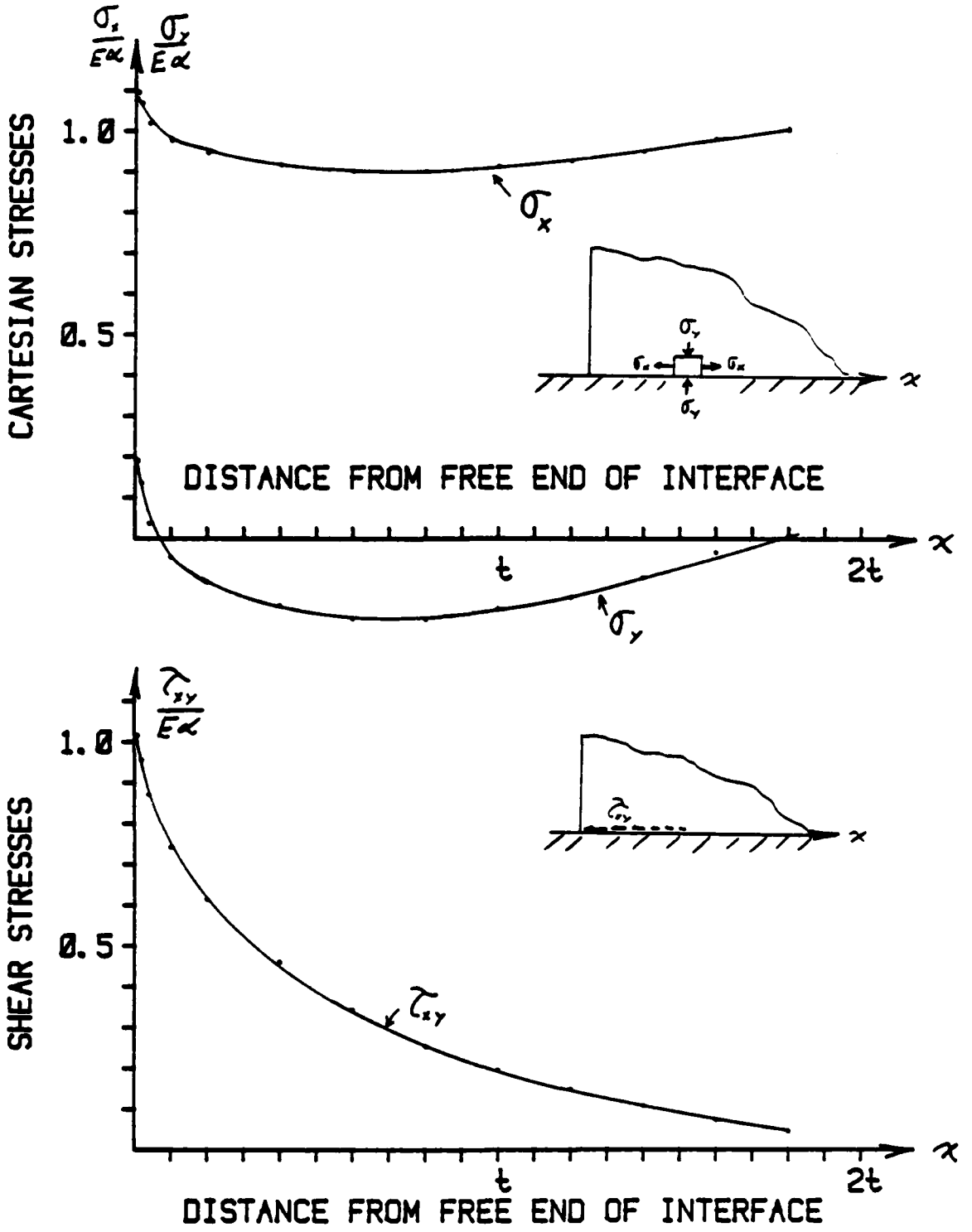

Fig. 5 — Cartesian and shear stresses along interface due to thermal shrinkage α

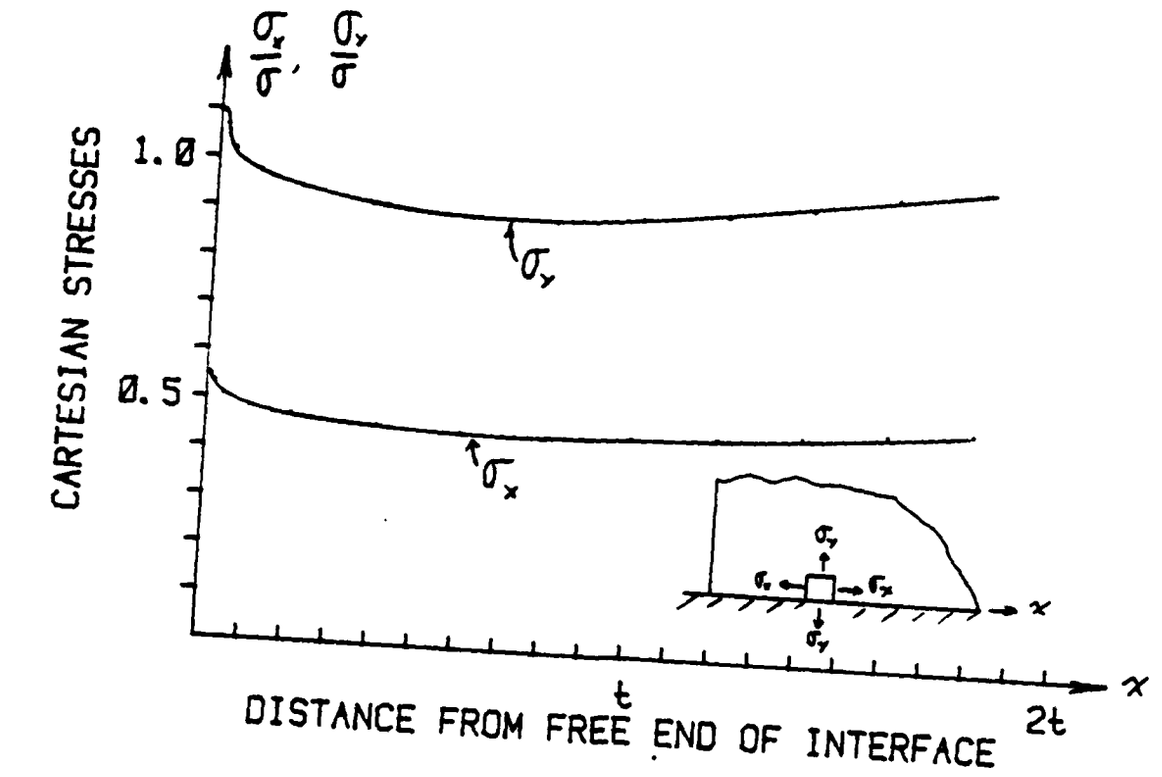

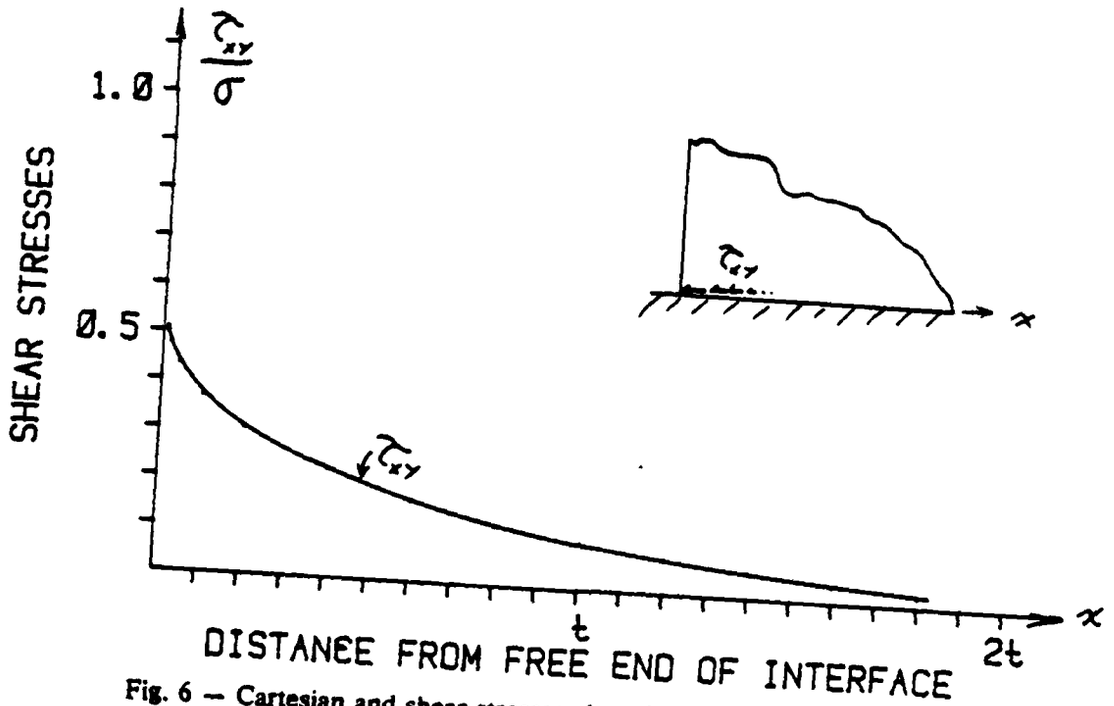

Fig. 6 — Cartesian and shear stresses along interface due to axial load σ

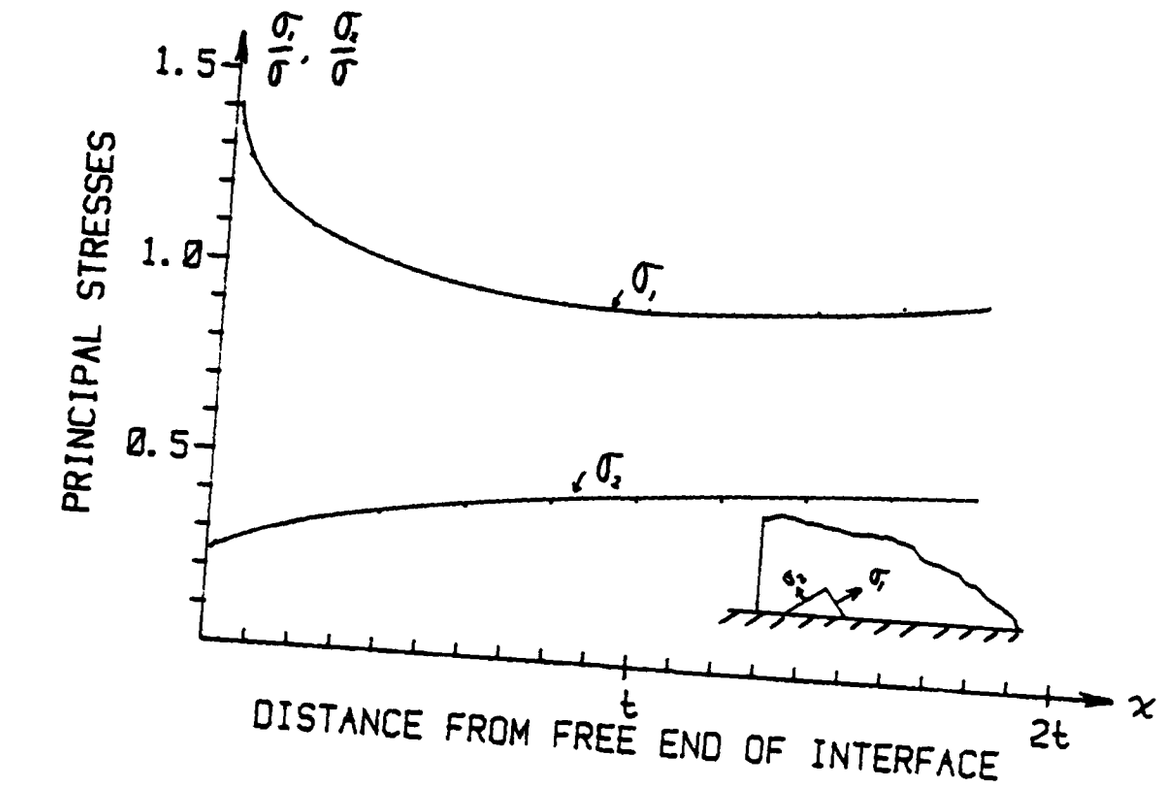

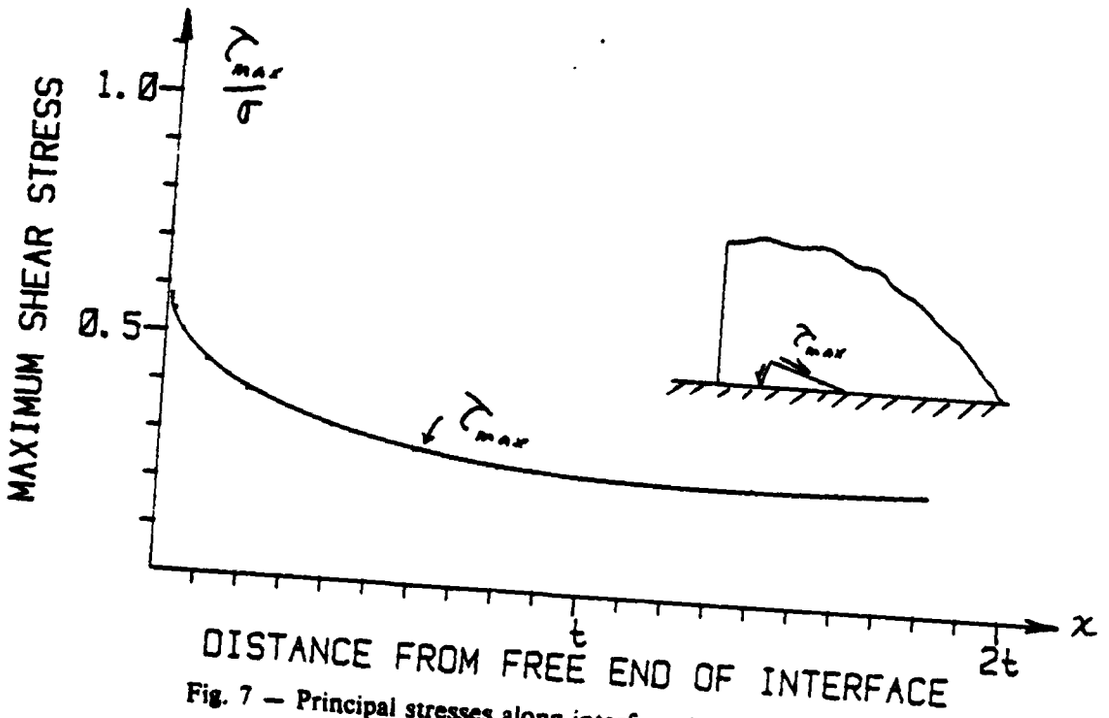

Fig. 7 — Principal stresses along interface due to axial load σ

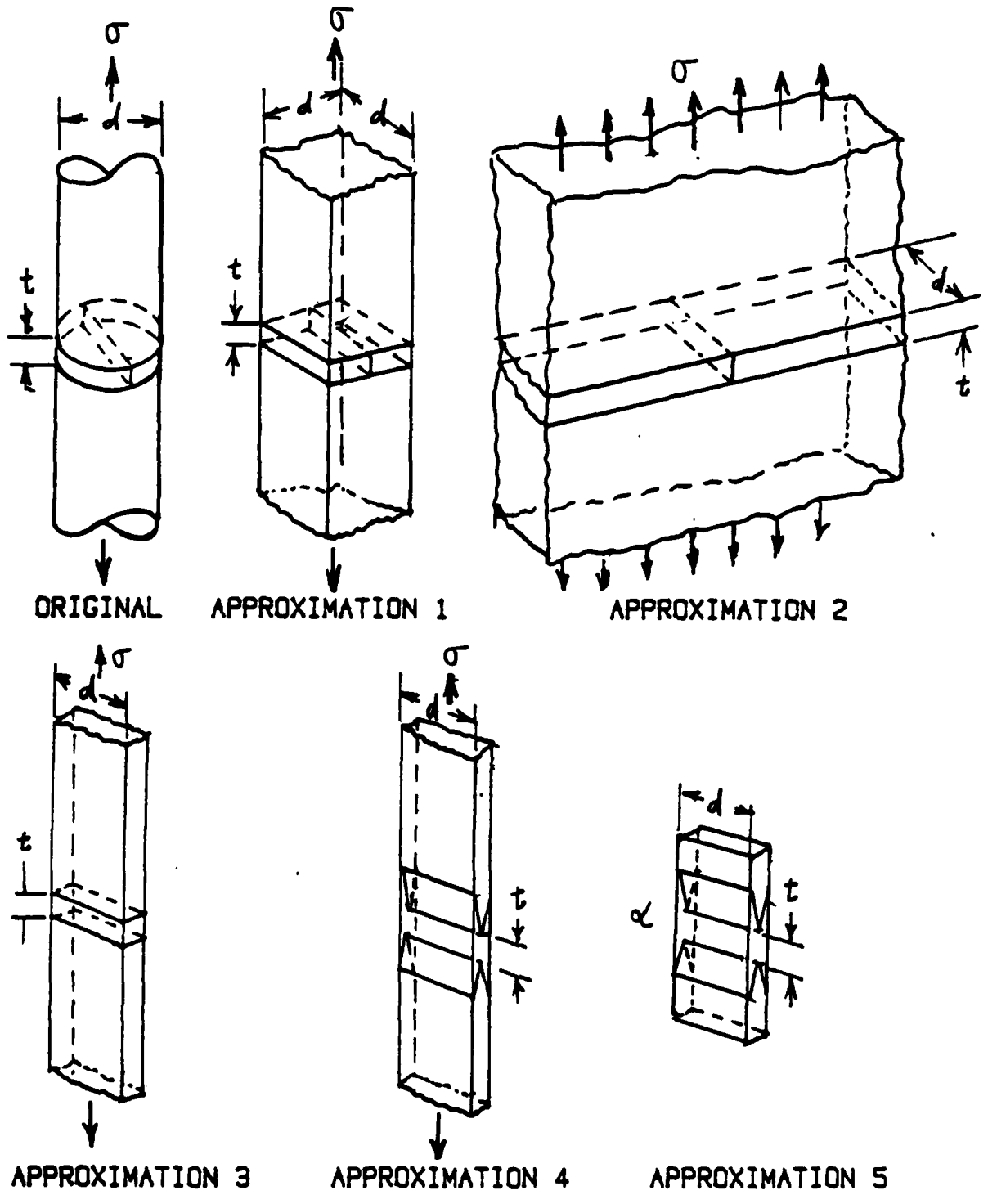

Fig. 8 — Series of approximations, from axisymmetric tension on a bar with a wafer, to thermal shrinkage on a two-dimensional strip

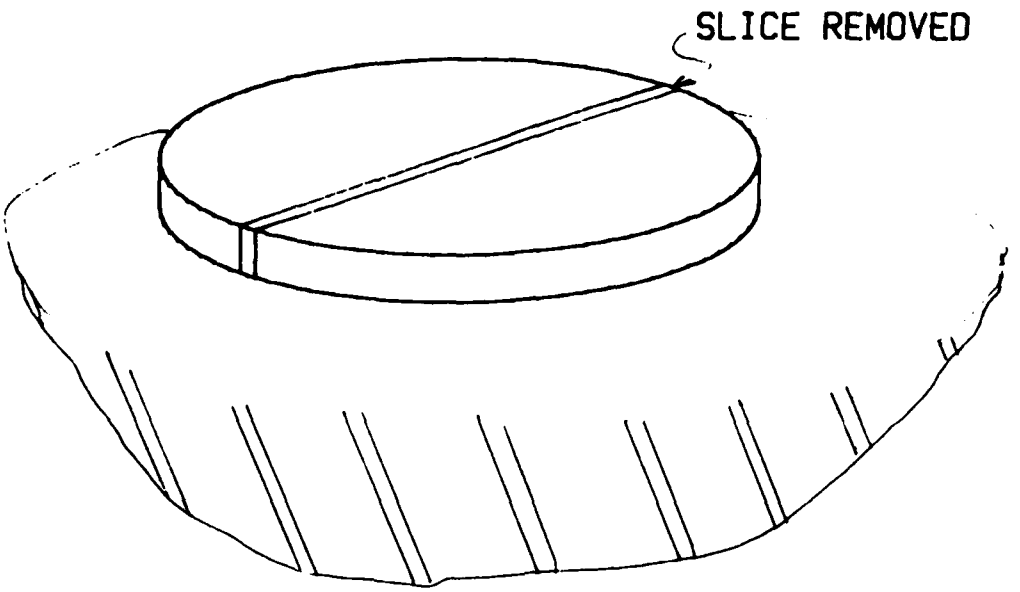

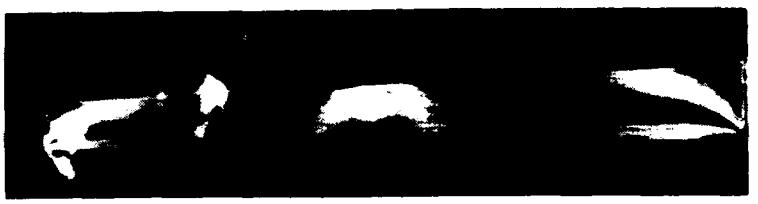

DARK FIELD

LIGHT FIELD

Fig. 9 — Isochromatic fringes on slice cut from bonded and shrunk wafer. The oval-shaped fringe at the top center of the slice is an unexplainable anomaly, but does not seem to effect the pattern near the corners.

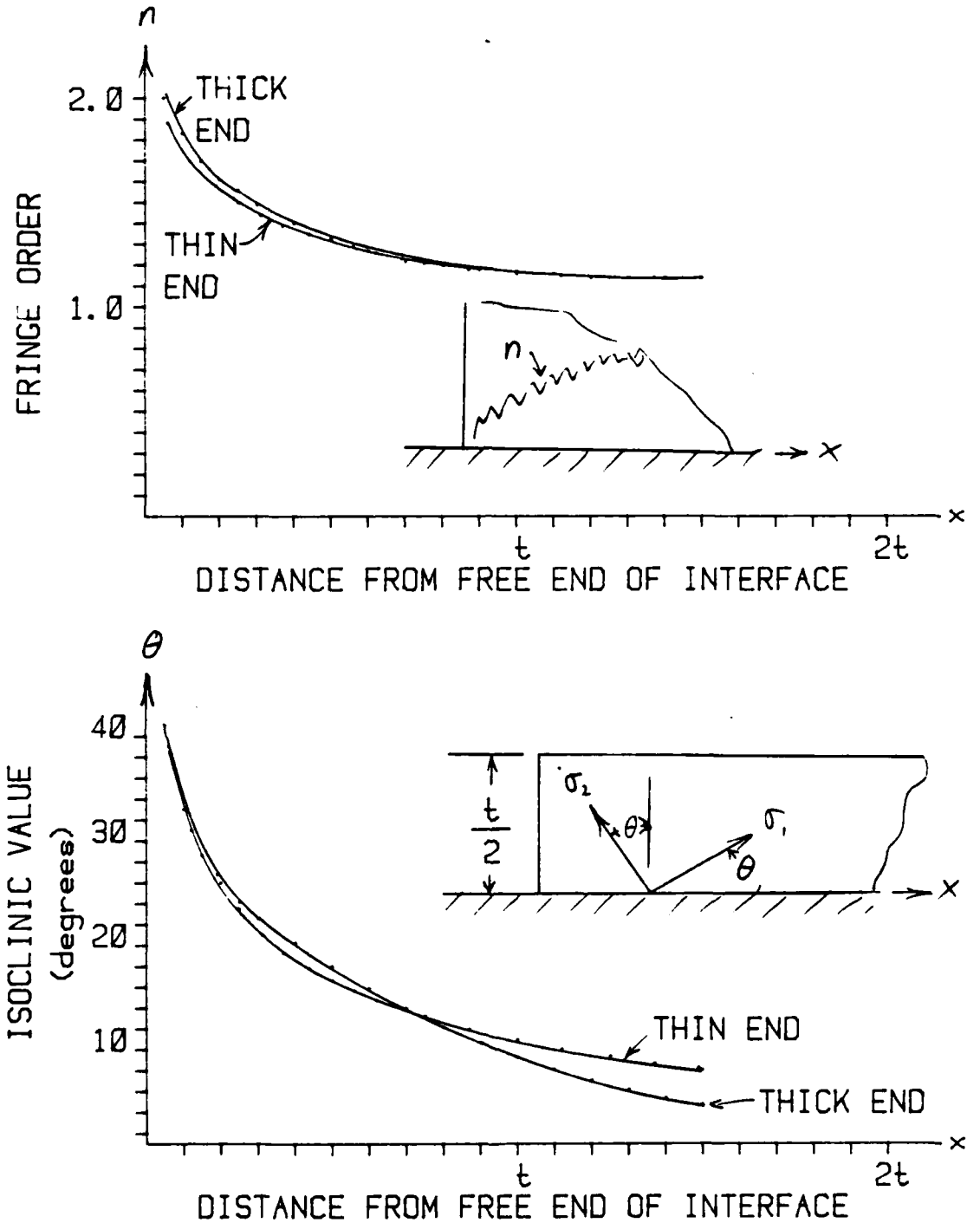

Fig. 10 — Isochromatic fringes and isoclinic values along 3D model interface near free edge. Isoclinics show the direction of the principal stresses.

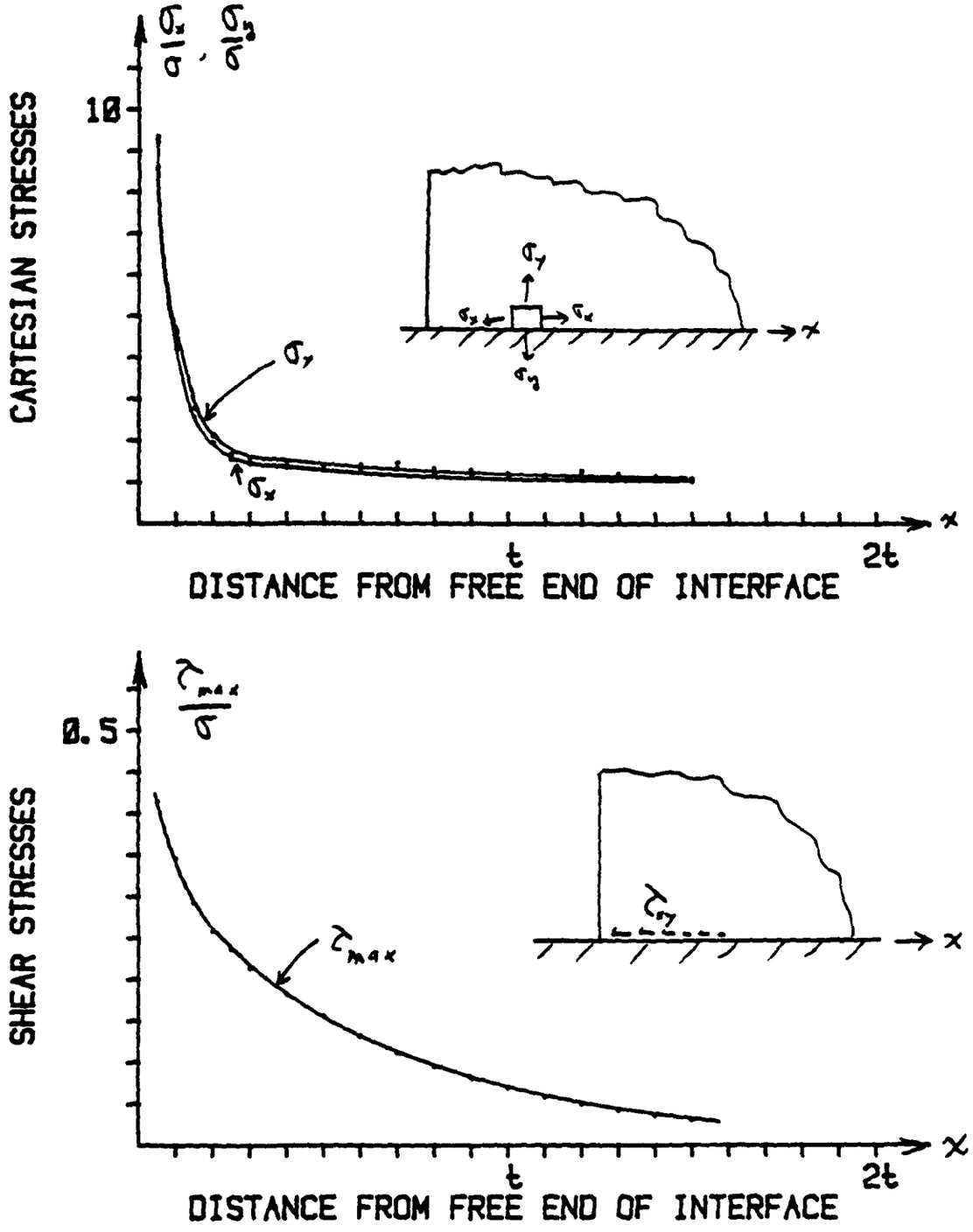

Fig. 11 — Cartesian and shear stresses along interface due to axial load σ (thick end)

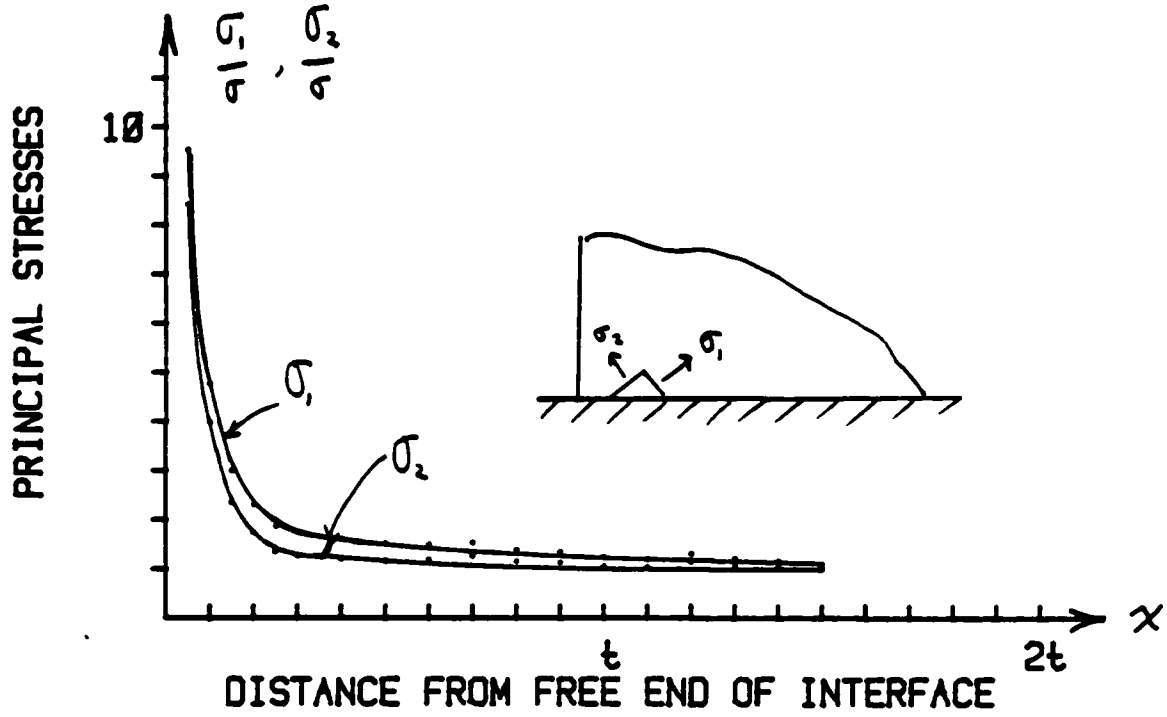

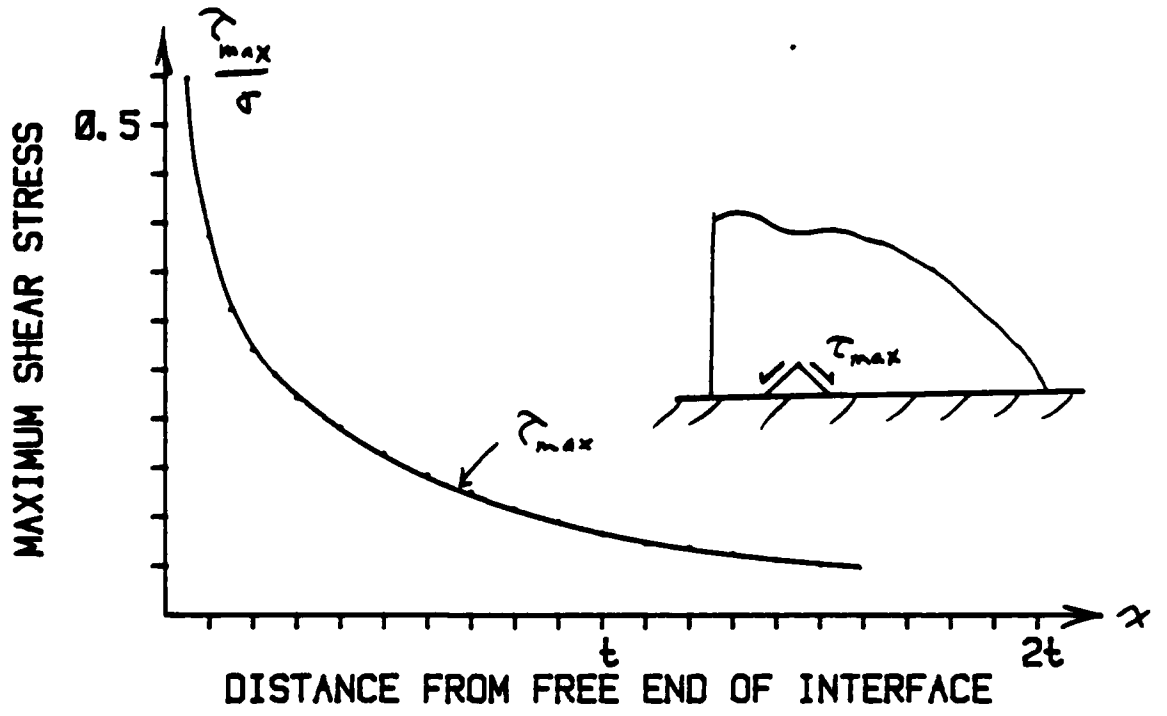

Fig. 12 — Principal stresses along interface due to axial load σ

Appendix

STRESSES ON A LOADED, BONDED INTERFACE

Probably the simplest, non-trivial example of stresses on a bonded interface subjected to load, is a specimen made of two circular rods, bonded and loaded with axial tension, as shown in Fig. A-1. The rods are assumed bonded to each other, without a bonding agent. A bonding agent would complicate the stress system. The rods are assumed to be of different materials, with different mechanical properties. If they have the same material properties, the stress system would reduce to the trivial case of uniform uniaxial stress throughout the two rods. Two material constants are sufficient to describe the pertinent material properties. Young's modulus, E, and Poisson's ratio, ν, are the most commonly chosen constant properties and will be used here.

The average vertical stress throughout the rods will be the force divided by the horizontal cross section. This stress will be termed σ and the subscripts 1 and 2 used to distinguish between the more rigid rod, 1, and less rigid rod, 2.

For simplicity, consider the loading divided into two steps. First step, the load is applied to both rods without bonding, so that both rods are stretched vertically and contract horizontally, both differently depending on their material properties. Second step, the interface surface of the more rigid rod is squeezed, and the interface surface of the less rigid rod is stretched until both surfaces coincide in the position they would have physically due to the loading.

The stress due to the first part of the loading will be $\sigma = \sigma_1 = \sigma_2$ <u>everywhere</u> in both rods. That is, the actual stress everywhere on the rods will be the average stress.

Stresses due to the second step of the load will combine with the stresss due to the first step. These additional stresses will occur only on or near the interface.

From the theory of elasticity, the vertical strains due to the first step of the load will be,

$$\varepsilon_{v_1} = \frac{\sigma_1}{E_1} \qquad \text{(A-1)}$$

$$\varepsilon_{v_2} = \frac{\sigma_2}{E_2} \qquad \text{(A-1)}$$

and the horizontal strains of contraction due to the first step of load will be

$$\varepsilon_{h_1} = -\nu_1 \frac{\sigma_1}{E_1} \qquad \text{(A-2)}$$

$$\varepsilon_{h_2} = -\nu_2 \frac{\sigma_2}{E_2}$$

If $\Delta\varepsilon$ is defined as the difference in these two horizontal strains, as illustrated in Fig.A-2, it can be written,

$$\Delta\varepsilon = \varepsilon_{h_1} - \varepsilon_{h_2} \qquad \text{(A-3)}$$

$$\text{or } \Delta\varepsilon = (-\nu_1 \frac{\sigma_1}{E_1}) - (-\nu_2 \frac{\sigma_2}{E_2}) = \sigma (\frac{\nu_2}{E_2} - \frac{\nu_1}{E_1})$$

In the second step of loading, the interface surface of the more rigid material, 1, must be "pinched-in" to mate with the interface surface of the less rigid material, 2, which must be "stretched-out". This is illustrated in Fig. A-3.

If ε_{s_1} is defined as the negative horizontal pinching strain of the more rigid material, and ε_{s_2} is defined as the positive horizontal stretching strain of the less rigid material

$$\varepsilon_{s_2} - \varepsilon_{s_1} = \Delta\varepsilon = \sigma (\frac{\nu_2}{E_2} - \frac{\nu_1}{E_1}) \qquad \text{(A-4)}$$

Both the pinching and stretching act to produce horizontal stresses in all directions but no vertical stresses, except near the edges. Hooke's law for the "plane stress", uniform, biaxial, horizontal stress can be written,

$$\sigma_h = \frac{E}{1-\nu} \varepsilon_h$$

For the hard and soft materials,

$$\sigma_{h_1} = \frac{E_1}{1-\nu_1} \varepsilon_{s_1}$$

$$\sigma_{h_2} = \frac{E_2}{1-\nu_2} \varepsilon_{s_2} \qquad \text{(A-5)}$$

Both these horizontal stress fields must be in balance with horizontal shear force acting on the respective interfaces. The horizontal forces on the interfaces are equal, but act in opposite directions on each material, thus the horizontal stresses must be equal in magnitude, but opposite in sign.

$$\sigma_{h_1} = - \sigma_{h_2} \qquad \text{(A-6)}$$

Combining Eqns. (5) and (6)

$$\varepsilon_{s_1} = - \frac{E_2}{E_1} \frac{(1-\nu_1)}{(1-\nu_2)} \varepsilon_{s2}$$

$$\varepsilon_{s2} = - \frac{E_1}{E_2} \frac{(1-\nu_2)}{(1-\nu_1)} \varepsilon_{s1} \qquad \text{(A-7)}$$

Combining Eqns. (A-7) and (A-4) gives the horizontal strain in terms of the applied stress and the elastic constants.

$$\varepsilon_{s1} = -\sigma \left(\frac{\nu_2}{E_2} - \frac{\nu_1}{E_1}\right) \Big/ \left(1 + \frac{E_1}{E_2} \frac{(1-\nu_2)}{(1-\nu_1)}\right)$$

(A-8)

$$\varepsilon_{s2} = \sigma \left(\frac{\nu_2}{E_2} - \frac{\nu_1}{E_1}\right) \Big/ \left(1 + \frac{E_2}{E_1} \frac{(1-\nu_1)}{(1-\nu_2)}\right)$$

Substituting Eqn. (A-8) into Eqn. (A-5) gives the complete horizontal stresses in both materials,

$$\sigma_{h1} = \frac{-E_1}{1-\nu_1} \sigma \left(\frac{\nu_2}{E_2} - \frac{\nu_1}{E_1}\right) \Big/ \left(1 + \frac{E_1}{E_2} \frac{(1-\nu_2)}{(1-\nu_1)}\right)$$

(A-9)

$$\sigma_{h2} = \frac{E_2}{1-\nu_2} \sigma \left(\frac{\nu_2}{E_2} - \frac{\nu_1}{E_1}\right) \Big/ \left(1 + \frac{E_2}{E_1} \frac{(1-\nu_1)}{(1-\nu_2)}\right)$$

After some algebra the equations can be written,

$$\frac{\sigma_{h1}}{\sigma} = \frac{\nu_1 - (E_1/E_2)\,\nu_2}{1-\nu_1 + (E_1/E_2)(1-\nu_2)}$$

(A-10)

$$\frac{\sigma_{h2}}{\sigma} = \frac{\nu_2 - (E_2/E_1)\,\nu_1}{1-\nu_2 + (E_2/E_1)(1-\nu_1)}$$

Note that the two equations are the same, with an exchange of subscripts. This indicates that the same equation can be used to express horizontal stresses in both the more rigid and less rigid materials. In Fig. A-4, the expression is plotted for selected and equal Poisson's ratios, over the complete range of ratios of Young's modulus. Fig. A-5 shows an example of stresses due to different values of Poisson's ratio. Fig. A-6 shows stresses in two materials with a ratio of Young's modulus of 3, over the whole range of Poisson's ratios. Fig. A-7 shows stresses in two materials with the same modulus for all values of Poisson's ratio.

These equations illustrate the complexity of stress around even the simplest interface of two different materials. The additional stresses and strains are caused primarily by the difference of Young's modulus, and to a much lesser extent due to the difference in Poisson's ratio.

ADDITIONAL COMMENTS

EDGE EFFECT

The pinching and stretching strains that are analyzed occur on the interface and are average strains over the whole interface and do not apply near the free edge of the interface. On or near the free edge of the interface, stresses, primarily tensile and shear, build up. These stresses also depend on the ratio of properties and can be many times higher than the average stresses due to the load.

TEMPERATURE EFFECT

A similar state of stress can occur without load, due to just temperature, if the materials have a difference in their coefficients of thermal expansion, $(\alpha_1 - \alpha_2)$. If an increase in temperature is termed ΔT, then the expression on the right side of Eqn. (A-4) can be replaced by $(\alpha_1-\alpha_2)\,\Delta T$, and a development similar to that shown above leads to the horizontal stresses due to an increase in temperature,

$$\sigma_{h_1} = - \frac{(\alpha_1-\alpha_2)\,\Delta T\, E_1 E_2}{E_2\,(1-\nu_1) + E_1(1-\nu_2)} \qquad (A\text{-}11)$$

$$\sigma_{h_2} = \frac{(\alpha_1-\alpha_2)\,\Delta T\, E_1 E_2}{E_2\,(1-\nu_1) + E_1(1-\nu_2)}$$

This observation is useful in the experimental stress analysis of bonded materials, using the stress-freezing technique of three-dimensional photoelasticity. Since temperature changes occur in the test, if there is sufficient differential contraction during the stress-freezing portion of the temperature range, the resultant frozen stress pattern in the thermally loaded body without mechanical load can be used to represent the stress in the mechanically loaded body with the simple addition of the average uniform stress.

THE WAFER PROBLEM

The case of two circular rods of the same material separated by, but bonded to, a wafer of the same diameter but of a different material is analyzed exactly as given above. In this case, there are two interfaces which respond similarly to the interface described in the first example. All the above equations apply. This loading can also be simulated by differential thermal contraction.

There is a difference in the interpretation of the equations. In this case the whole wafer is near the interfaces, and so practically all the material of the wafer is pinched or stretched. Where the wafer is made of the less rigid material, this can lead to triaxial tension stresses throughout the central region of the wafer. If the wafer has a Poisson's ratio of near 0.5, the triaxial tension can approach a state of hydrostatic tension.

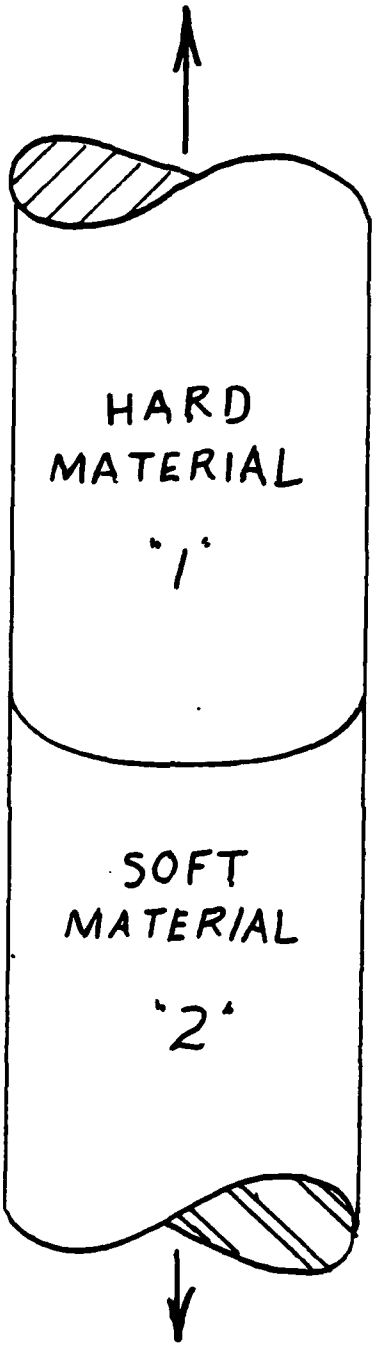

Fig. A-1 — Two circular rods of different materials bonded together and subjected to an axial tensile load

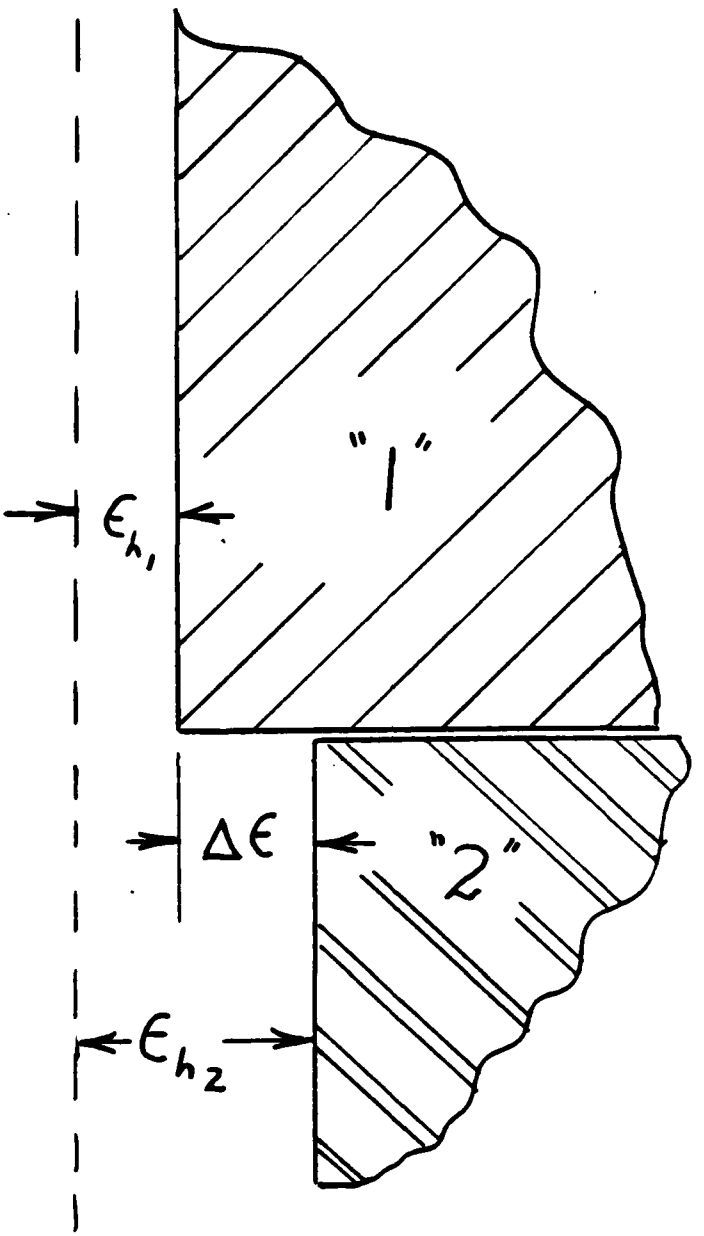

Fig. A-2 — A section at the corner of the intersection of two rods with unit radii showing the difference in the horizontal strains of diametral contraction after the first step of loading

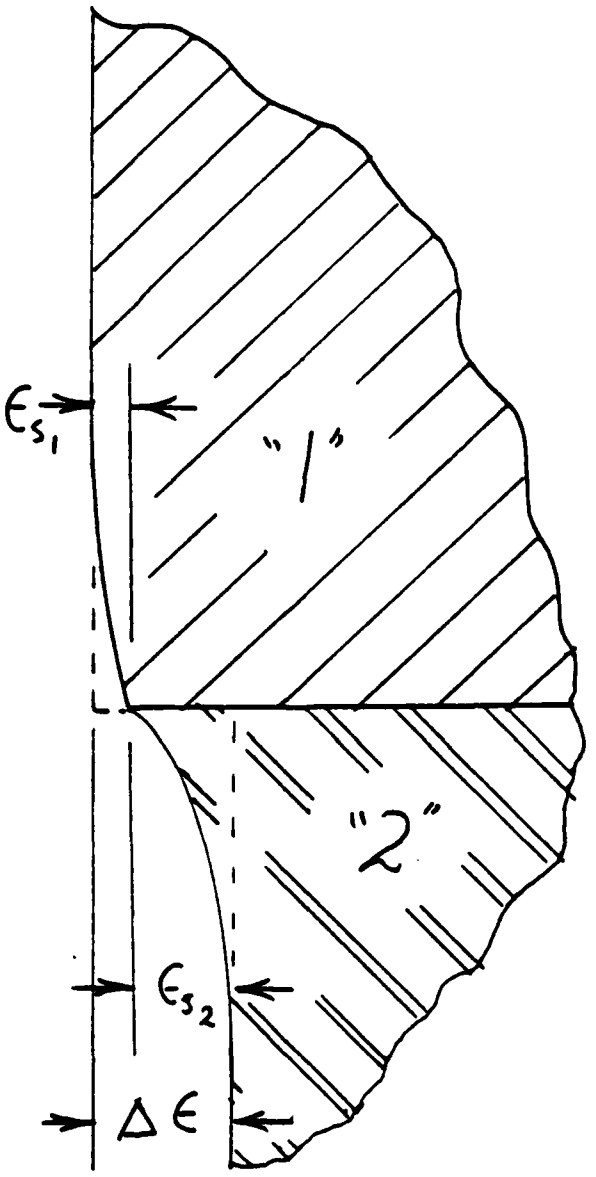

Fig. A-3 — The final deformed shape of the section in Fig. A-2 showing the pinching strain on the hard material (ϵ_{s_1}), the stretching strain on the soft material (ϵ_{s_2}), and how they are apportioned over $\Delta\epsilon$

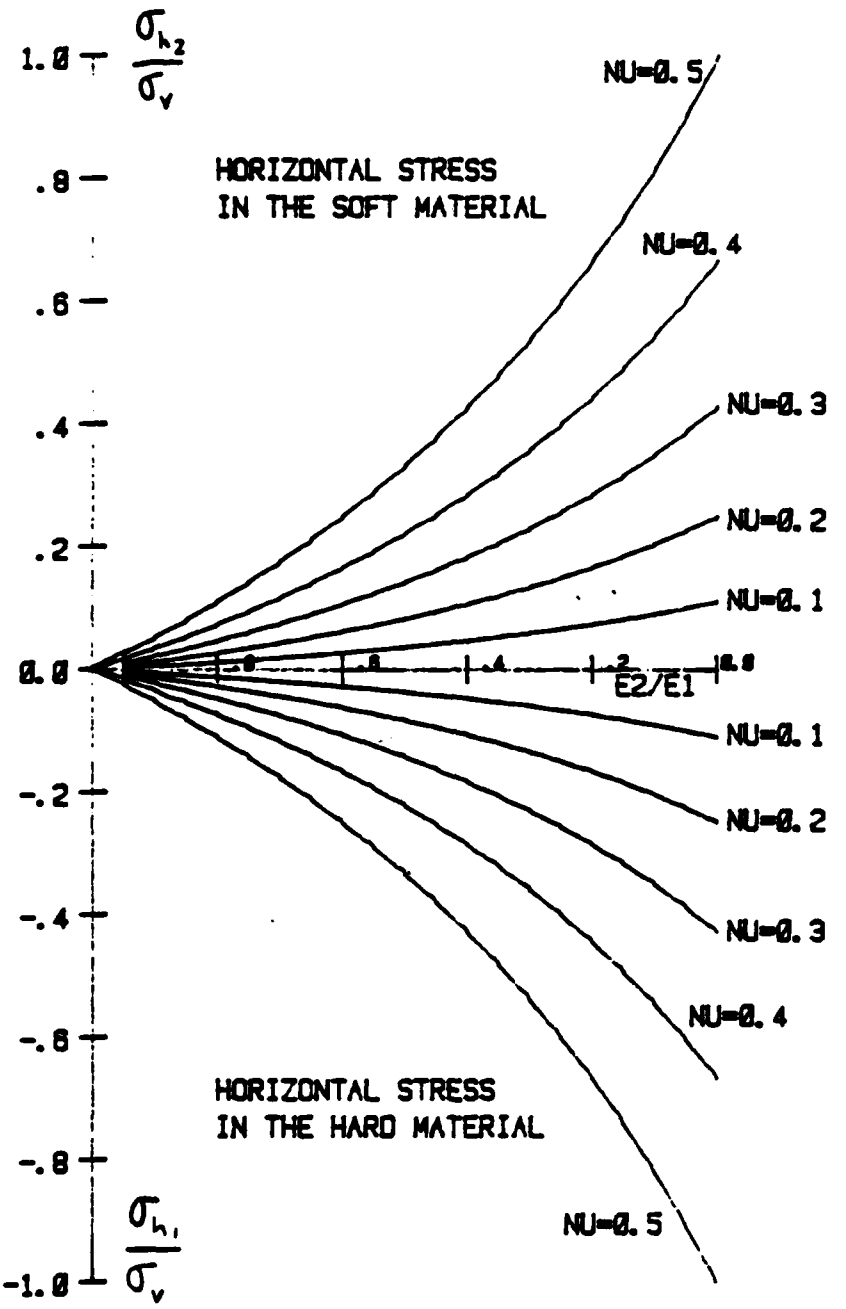

Fig. A-4 — Ratio of horizontal stress to vertical stress in the central region of an interface of two materials under load, for all combinations of Young's moduli and Poisson's ratios for which the Poisson's ratios are equal

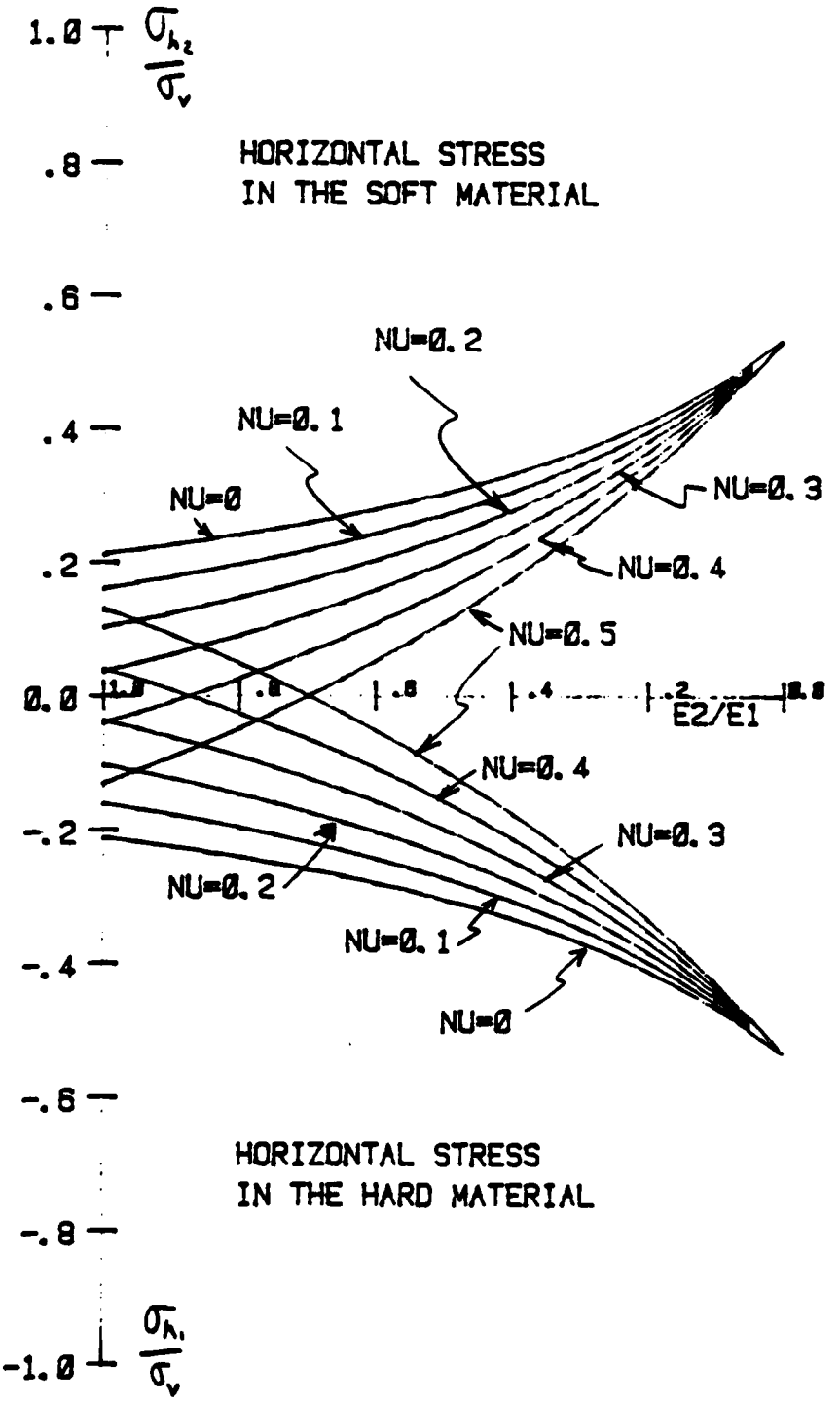

Fig. A-5 — Ratio of horizontal stress to vertical stress in the central region of the interface of two materials under load, for all combinations of Young's moduli and all Poisson's ratios of the hard material (NU) with Poisson's ratio equal to 0.35 in the soft material

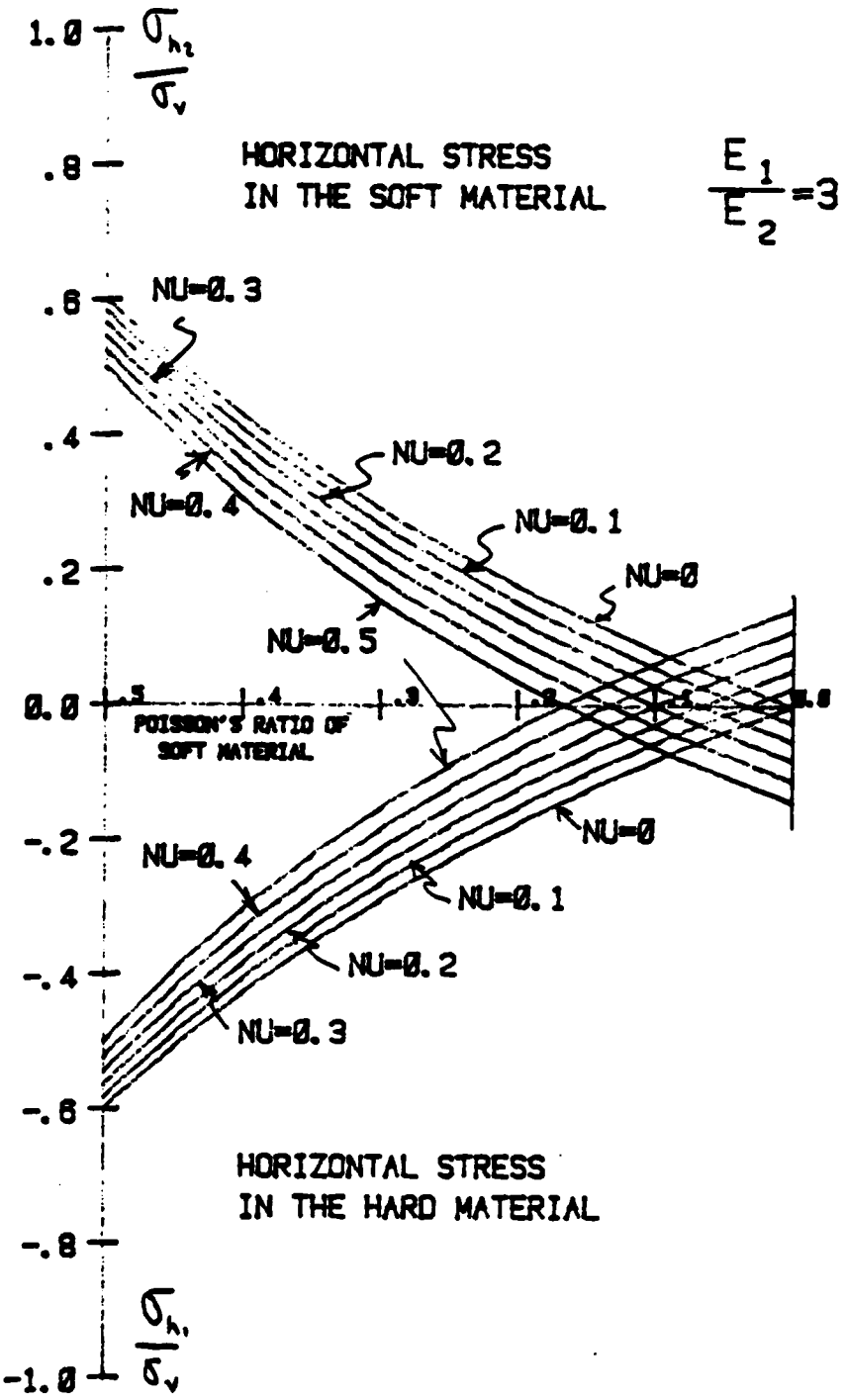

Fig. A-6 — Ratio of horizontal stress to vertical stress in the central region of an interface of two materials under load, for a Young's modulus ratio equal to 3 (1/3) and the full range of Poisson's ratios for isotropic materials (0 to 0.5)

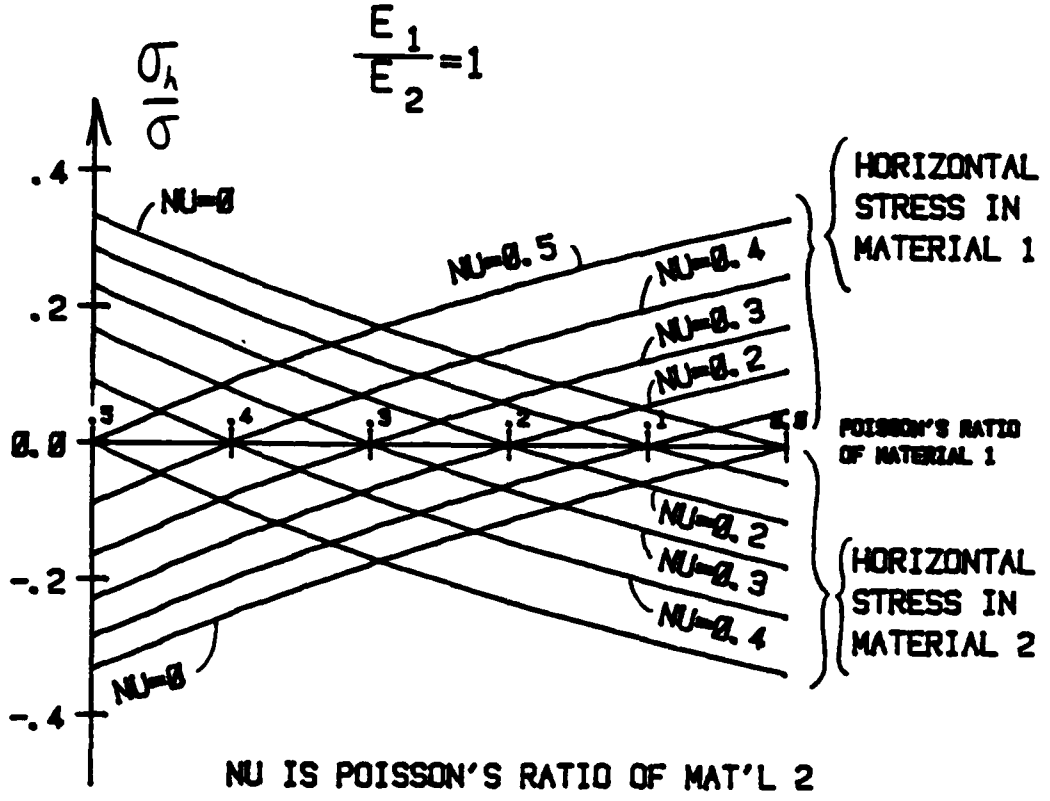

Fig. A-7 — Ratio of horizontal stress to vertical stress in the central region of an interface of two materials under load. The two have the same Young's modulus.

END

DTIC

9-86